would appear that Eq. [3] or [4] may be used to give fairly precise pressures for given temperatures

$$\log pO_2 = 6.48773 - 2996.83/T; \quad \text{s.d.} = 0.02731 \quad [1]$$

$$\log pO_2 = -2493.13/T + 2.02688 \log T; \quad \text{s.d.} = 0.03709 \quad [2]$$

$$\log pO_2 = 94.6148 - 7438.44/T + 0.00991043T - 31.1855 \log T; \quad \text{s.d.} = 0.01281 \quad [3]$$

$$\log pO_2 = -292.9857 + 5301.69/T - 0.102885T + 120.944 \log T + 0.000031697T^2; \quad \text{s.d.} = 0.01278 \quad [4]$$

The least squares analyses in this paper were carried out on the National Bureau of Standards electronic computer, using the appropriate OMNITAB Program (12).

Conclusions

A study of the Ag_2O-Ag-O_2 system has been completed, overlapping the work of Benton and Drake, and closing the gap which existed between the temperature ranges used by Benton and Drake, and Lewis. It can now be said that the system has been studied from 446°K, the lowest temperature used by Benton and Drake, to 773°K, the highest temperature used by Keyes and Hara. All data have been included in the present determination of the thermodynamic constants.

Acknowledgment

The author wishes to express his gratitude to Dr. W. J. Hamer for his continued interest in the investigation.

Manuscript received Feb. 8, 1966. This paper was presented at the Buffalo Meeting, Oct. 10-14, 1965.

Any discussion of this paper will appear in a Discussion Section to be published in the June 1967 JOURNAL.

REFERENCES

1. H. LeChatelier, *Z. physik. Chem.*, **1**, 516 (1887).
2. G. N. Lewis, *J. Am. Chem. Soc.*, **28**, 139 (1906).
3. F. G. Keyes and H. Hara, *ibid.*, **44**, 479 (1922).
4. A. F. Benton and L. C. Drake, *ibid.*, **54**, 2186 (1932).
5. E. M. Otto, *This Journal*, **111**, 88 (1964).
6. E. M. Otto, *ibid.*, **112**, 367 (1965).
7. J. Hilsenrath, U. S. Nat'l. Bur. Standards Circular 564 (1955).
8. K. S. Pitzer and W. V. Smith, *J. Am. Chem. Soc.*, **59**, 2633 (1937).
9. K. K. Kelley, U. S. Bur. Mines Bull., 584 (1960).
10. K. Kobayashi, *Sci. Rep. Tohoku Univ.*, (I) **35**, 173 (1951).
11. D. D. Wagman, U. S. Nat'l Bur. Standards Technical Note, 270-1 (1965).
12. J. Hilsenrath, G. G. Ziegler, C. G. Messina, P. J. Walsh, and R. J. Herbold, U. S. Nat'l Bur. Standards Handbook 101 (in press).

Studies of Hydrocarbon Fuel Cell Anodes by the Multipulse Potentiodynamic Method

II. Behavior of Methane on Conducting Porous Teflon Electrodes

L. W. Niedrach

General Electric Company, Research and Development Center, Schenectady, New York

ABSTRACT

Rates of adsorption of methane on semimicro Teflon-bonded, platinum black fuel cell electrodes in the presence of a perchloric acid electrolyte are about an order of magnitude lower than those previously observed with ethane. At 65°C the measured rate of adsorption on a clean surface correlates well with the maximum anodic current that can be drawn from the electrode. The ad-layer on the surface of the electrode consists of C_1 species, some of which are partially oxidized. Similar C_1 species which form upon the adsorption of higher molecular weight hydrocarbons appear to play an important role in the over-all anodic oxidation of hydrocarbons. This implies that an efficient catalyst for hydrocarbon anodes should promote the cracking of higher molecular weight hydrocarbons to form C_1 radicals and also promote the reaction of these fragments with water.

The behavior of ethane and related hydrocarbons on smooth platinum electrodes in the presence of a perchloric acid electrolyte has been investigated with the multipulse potentiodynamic (MPP) method in this laboratory (1, 2). Recently the method has been extended to porous fuel cell anodes of more complex structure with which the behavior of ethane was examined in detail; a few preliminary experiments were performed with methane and propane (3). For this purpose a miniature version of a previously described (4) conducting-porous-Teflon fuel cell electrode (containing platinum black as catalyst) was employed.

This work showed that the behavior of ethane on the Teflon-bonded electrodes is both mechanistically and kinetically similar to that on smooth platinum (3). It also indicated that ethane and propane are similar in that their ad-layers on the electrode surface show two oxidation waves when a linear anodic sweep (l.a.s.) is applied. The first wave occurs at potentials below which (approximately 0.8v) the electrode surface is itself oxidized. This first wave generally exhibits a well-defined peak. The second wave is more diffuse and extends all the way from approximately 0.8v to oxygen-evolution potentials. Methane was found to differ markedly, however, in that only one wave could be detected during oxidation of its adlayer. Because this wave corresponded to that of the more readily oxidized species from ethane and propane, it was felt desirable to investigate the behavior of methane in greater detail.

As in the previous study of ethane, a perchloric acid electrolyte was employed over a range of temperatures. Particular attention was given to the rates of adsorption and the nature of the species that form on the surface of the electrode. In addition data were again obtained to relate these properties to the over-all polarization curve for the fuel electrode.

Experimental

The equipment and general procedures utilized in these investigations have been described previously (3). In brief, the 0.2-cm diameter Teflon-bonded, platinum black electrode was mounted in a three-compartment, Teflon cell. Platinized platinum flags served as the hydrogen reference and counter electrodes. The former communicated with the working anode through

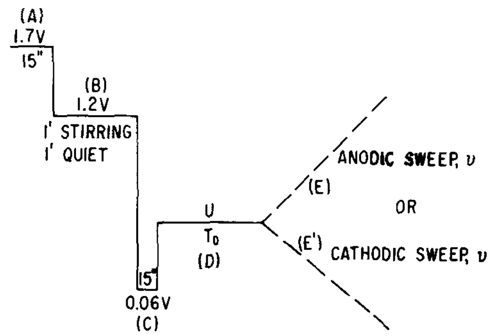

Fig. 1. Potential sequences applied to the test electrode

a Luggin capillary. The cell was operated in an air thermostat enabling control of the temperature to within 0.1°C.

The 4.3N perchloric acid electrolyte solution used for this work was prepared from reagent grade perchloric acid and quartz distilled water. Electrolytic grade hydrogen was used in the reference electrode chamber, and Phillips research grade methane was used as the fuel. Tank argon, deoxygenated by passage over heated copper turnings, was used as the "fuel" for obtaining solvent blanks. Tank argon was also used for degassing the solution.

The electronic instrumentation and circuit have been described previously (5).

The potential-time sequence applied to the anode for adsorption studies at constant potential is shown in Fig. 1. The rationale behind the various steps has been discussed in detail elsewhere (1-3, 5). Briefly, however, steps A through C serve to precondition the electrode and return it to a reproducible state before each equilibration. Following oxidation of impurities during step A, the electrode is taken to step B to allow the system to become quiescent while adsorption of fuel is prevented by an "adsorbed oxygen" layer on the electrode. In step C the oxygen layer is reduced at a potential sufficiently low that fuel adsorption is still prevented. Upon shifting to the potential of step D fuel adsorption occurs for the allotted time, T_D. Anodic sweep E is then applied to determine the charge required for the oxidation of the fuel ad-layer. The alternative cathodic sweep E' is used to determine the "real" surface area of the electrode from the charge corresponding to hydrogen deposition. In this case, argon is substituted for the fuel.

For the present electrode the useful range of sweep speed v for oxidation of the ad-layer was previously established by adsorbing a fixed amount of ethane (corresponding to $T_D = 600$ sec) and measuring the charge required for its oxidation over a range of sweep speeds (3). The useful range was found to extend from approximately 0.1 to 0.4 v/sec. Lower sweep rates resulted in additional charge from the oxidation of fuel that adsorbed during the sweep. At higher sweep rates the traces tended to lose definition, because of the diffuse structure of the electrode. A sweep speed of $v = 0.1$ v/sec was used routinely in the present work.

Steady-state polarization curves such as that in Fig. 7 were obtained in two ways. The first method involved application of steps (A-D) of Fig. 1 before each measurement of current at a particular potential U. Ten-minute equilibrations were allowed on each point before the final value of current was recorded. In the second method, steps (A-D) of Fig. 1 were applied only once, at the lowest value of U. The potential was then changed in increments and the current recorded for each potential after an apparent constant value was established. The two methods gave essentially identical results.

Results

The general form of the current-voltage trace obtained during oxidation of adsorbed methane with a

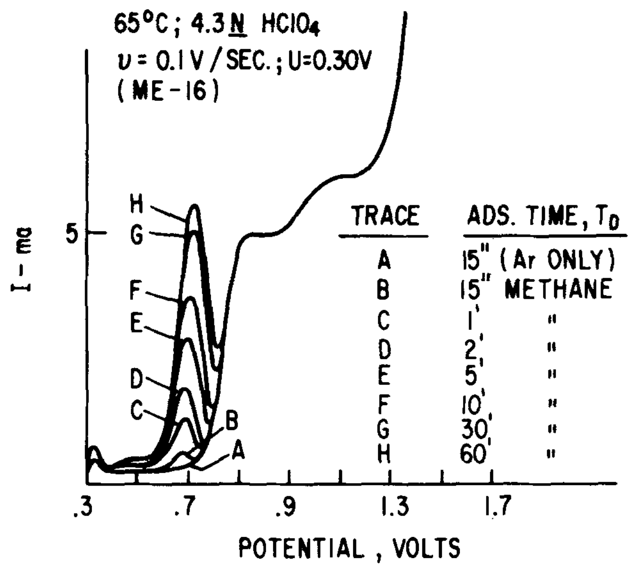

Fig. 2. Current-potential (time) traces for methane after different adsorption times.

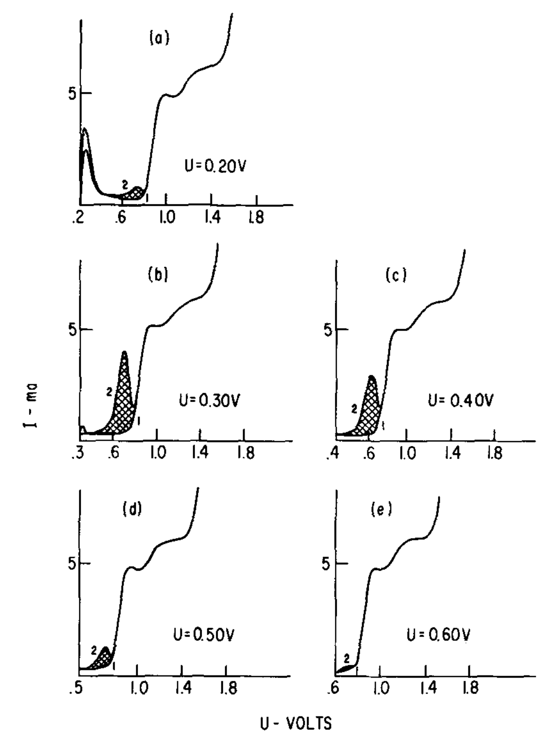

Fig. 3. Current-potential (time) traces for methane adsorbed at several potentials. 4.3N $HClO_4$; 65°C; $V = 0.1$ v/sec; $T_D = 10$ min; 1, Ar blank; 2, methane; ME-16.

linear anodic sweep is shown for a range of equilibration times, potentials, and temperatures in Fig. 2-4. For each experimental condition a trace corresponding to the background solvent blank is also presented. Figure 2 shows a series of traces for adsorbed methane at 65°C for various equilibration times at a potential of 0.3v. The effect of the equilibration potential at 65°C appears in Fig. 3. Similar data showing the effect of temperature appear in Fig. 4. In obtaining the data for the latter two figures 10-min equilibrations were used throughout.

It is clear from Fig. 2-4 that the amount of methane adsorbed is a strong function of the time, potential, and temperature. However, for all conditions of potential and temperature and for equilibration times as long as an hour only the single wave is obtained during oxidation of the ad-layer. This wave, like wave 1 for ethane (3), becomes more prominent as the tem-

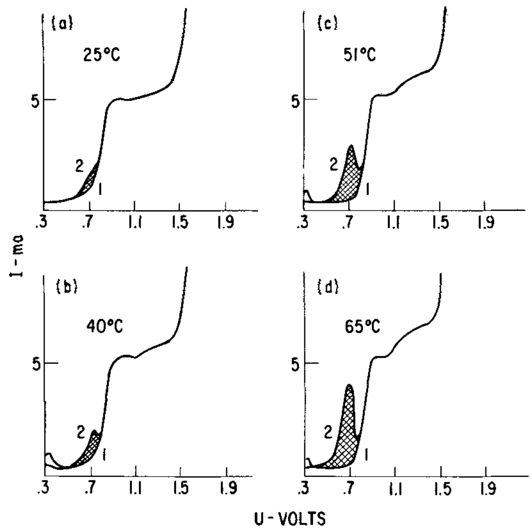

Fig. 4. Current-potential (time) traces for methane adsorbed at several temperatures. 4.3N $HClO_4$; V = 0.1 v/sec; T_D = 10 min; U = 0.3v; 1, Ar blank; 2, methane; ME-16.

perature is increased. Because the material is so readily oxidized it is no longer seen when equilibrations are performed as potentials greater than 0.5v.

The magnitude of the charge, Q_{E1},[1] associated with the oxidation of the material adsorbed after any time, T_D, was obtained by integrating the area enclosed by the solvent (blank) curve and the methane curve. This is indicated by the shaded areas in the figures. It is to be noted that hydrogen formed by dissociation during the initial adsorption step is not included in these measurements.

Variations in Q_{E1} with time at different potentials are shown in Fig. 5 for equilibrations performed at 65°C. The data have been normalized to charge per unit of "real" surface area as determined by cathodic deposition of hydrogen on the electrode. A conversion factor of 0.21 mcoul/cm² was used in calculating the "real" area (6).

As in the case of ethane (3) the rate of adsorption is initially constant and then follows an empirical Elovich relationship over a moderate range. Ultimately a steady-state coverage is achieved when the rate of adsorption equilibrates with the rate of oxidation. At 65°C the maximum (initial) adsorption rate for methane in terms of $\Delta Q_{E1}/\Delta t$ is approximately 0.00030 mcoul/sec/cm² of real area.

[1] Q_{E_1} is used to designate this charge because the oxidation occurs in the same potential region as that of wave 1 for ethane and propane. In contrast to ethane and propane, however, $Q_{E_1} = Q_{E_{tot}}$ for methane; here $Q_{E_{tot}}$ is the charge required to oxidize all of the adsorbed surface species derived from the hydrocarbon fuel.

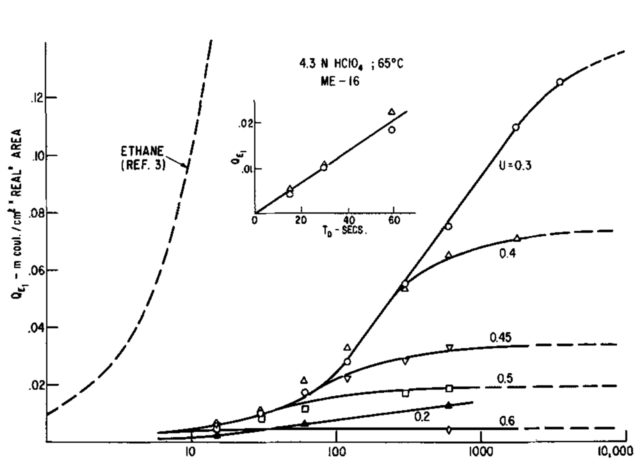

Fig. 5. Variation of surface charge with time for methane adsorbed at several potentials at 65°C.

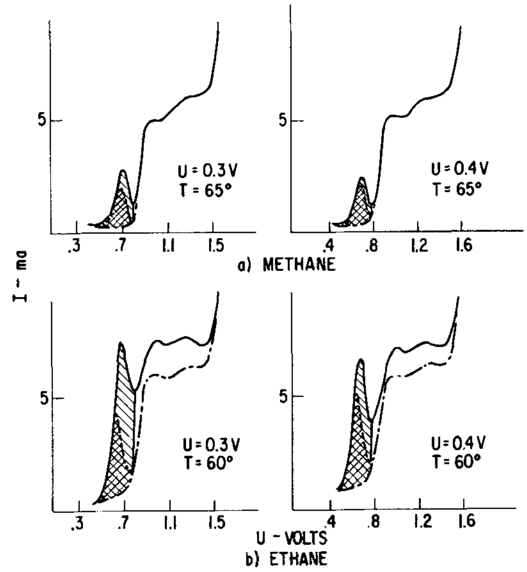

Fig. 6. Effect of cathodic hydrogenation on the current-potential (time) traces for adsorbed methane and ethane. 4.3N $HClO_4$; ——— initial; --- after hydrogenation; —·— argon blank; T_D = 5 min.

Because of the low rate, even at 65°C, detailed measurements of this type were not made at other temperatures. However, at 25°C Q_{E1} = 0.0088 mcoul/cm² of real area after a 10-min equilibration. At this low coverage it is to be expected that the adsorption would still be in the linear region. Using such an assumption one calculates a rate of 0.000015 mcoul/sec/cm² of real area, or a magnitude less than that at 65°C. This corresponds to an activation energy of about 15 kcal/mole. For ethane a similar temperature effect was found by direct measurement of the initial rates at 25° and 60°C (3). The observed rates at the two temperatures, which were 0.0010 and 0.010 mcoul/sec/cm² of real area, respectively, correspond to an activation energy of 13 kcal/mole.

The single wave for methane occurs in the same potential range as wave 1 for ethane and propane, as well as such partially oxygenated species as CO, formic acid and "reduced CO_2" (3). It therefore appears that similar surface species are involved in these cases. To determine whether some of the species of this wave for methane are removable by cathodic hydrogenation and therefore probably unoxygenated, cathodic hydrogenations were performed after equilibrations of the electrode with methane at 0.3 and 0.4v. In these experiments, sequence A-D of Fig. 1 was first followed. After adsorption for time, T_D, the potential was again stepped down to 0.06v for 2 to 5 min before application of the linear anodic sweep. Similar experiments were also performed with ethane for comparison. The results of these experiments are summarized in Fig. 6 and Table I. It is clear that in each case a portion of the surface species was removed by this treatment. The amount removed decreased with increasing equilibration potential. In the case of ethane all of wave 2 was removed by the hydrogenation treatment. The present results for ethane differ

Table I. Effect of cathodic hydrogenation on wave 1 (T_D = 5 min; T_{Hyd} = 5 min)

	Methane 65°C 0.3v	Methane 65°C 0.4v	Ethane 60°C 0.3v	Ethane 60°C 0.4v
Q_{E_1} = initial; mcoul	4.0	2.8	10.1	8.0
Q_{E_1} = after hydrogenation: mcoul	2.5	2.3	3.8	5.5
ΔQ_{E_1} mcoul	1.5	0.5	6.3	2.5
Per cent removed	38	18	62	31

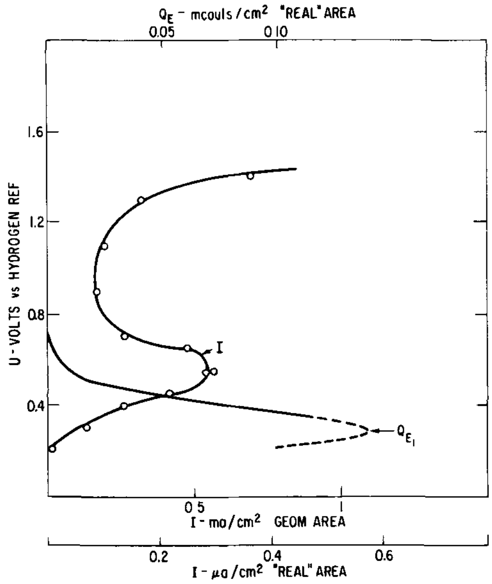

Fig. 7. Polarization and surface charge curves for methane. 4.3*N* $HClO_4$; T = 65°C; ME-16.

from those of Gilman (1) who performed similar hydrogenations with the wire microelectrode after equilibrations at 0.4v. In that case no desorption of wave 1 species was observed after hydrogenation at 0.06v. The diffuse structure of the Teflon electrode as well as small differences in the catalytic behavior may account for the observed differences.

One additional point for consideration is the relationship between the adsorption data and the polarization curve for the electrode operating on methane. Such a polarization curve obtained at 65°C is shown in Fig. 7. The abscissa is expressed in terms of the current density per unit of real and geometrical area of the electrode. Therefore the data may be related to the adsorption studies as well as performance curves for fuel cells. Also shown in the figure is the measured surface coverage, Q_{E1} as determined from linear anodic sweep measurements. The forms of the polarization and surface coverage curves are similar to those previously reported for ethane (3); however, the amplitudes of both are considerably less than for ethane.

Similar bell shaped curves relating surface coverage to potential have also been observed by others with platinum electrodes and a variety of fuels and electrolytes. For example such curves have been obtained electrochemically for ethane (1), ethylene (2) and acetylene (2) with a perchloric acid electrolyte, for methane (7), ethane (7), propane (7, 8) and butane (7) with a phosphoric acid electrolyte, and for ethane with a hydrofluoric acid electrolyte (7). Radiochemical tracer techniques have also given similar results for ethylene with a sodium hydroxide electrolyte (9) and a sulfuric acid electrolyte (10) and for butane with a sulfuric acid electrolyte (11).

Discussion

In considering the results for methane, it will be most useful to relate them to the previous observations with other fuels. As already noted, a most significant difference lies in the fact that but a single oxidation wave is obtained for the ad-layer from methane in contrast to the two waves from the ethane and propane. Gilman, after studies of ethane (1), ethylene (2), and acetylene (2) has concluded that wave 2 from ethane is associated with the oxidation of partially dehydrogenated C_2 species on the electrode surface. It is reasonable to conclude that similar multiple carbon species are associated with the second wave from propane and that a corresponding analogy will hold for higher hydrocarbons. With these higher molecular weight materials it is likely that a variety of species of different chain length will be present and contribute to the second wave. These would result from cracking and polymerization reactions which have been demonstrated to occur even at 25°C (12).

It has also been noted in past work that C_1 species are among the cracking products obtained from the higher hydrocarbons at 25° (12) and at 65°C (13). Furthermore, the cracking of propane on platinum in the absence of electrolyte has been observed to form methane and ethane and to have a pronounced temperature coefficient (14). In view of these observations and the fact that only wave 1 is observed with methane, it seems clear that the more readily oxidized surface material corresponds to C_1 species. Previous observations (1, 12) as well as the data in Table I and Fig. 6 indicate further that these species are partially oxygenated.

The adsorption rates and steady-state coverages for methane are considerably lower than those previously observed with ethane; however the variation in coverage with potential parallels that for ethane. With regard to the lower rate of adsorption for methane, this may relate to the somewhat higher dissociation energy required to break the first C-H bond than is required for ethane, 101-102 kcal *vs.* 97 kcal, respectively (15). Alternatively, it may reflect a weaker physical adsorption prior to dissociation on the surface to form the chemisorbed species. Sufficient detailed data are, however, unavailable at the present time to reach a definitive conclusion concerning the reason for the pronounced differences.

The shape of the curve relating surface coverage to potential reflects the influence of competing reactions. At low potentials (< 0.3v) adsorption is hindered because the required dissociation of the adsorbing hydrocarbon is repressed by the presence of atomic hydrogen on the electrode surface. At potentials above 0.3v the surface coverage again declines in order to permit the rate of adsorption to keep pace with the increasing rate of oxidation of the ad-layer. It is possible that the shape of the curve is further influenced by a potential-dependent, competitive adsorption with water which has been used in the interpretation of the effect of potential on the adsorption of ethylene (10).

The low adsorption rates for methane are reflected in the low current densities obtained with methane as seen in the polarization curve of Fig. 7. The maximum current density, at 0.5v, is about one tenth that obtained with ethane. In this connection it is of interest to relate the maximum current density to the adsorption rates on the clean surface, *e.g.* the initial rates at 0.3 and 0.4v.

To convert the adsorption rates to equivalent current densities, it must be recalled that the former are expressed in terms of the change in surface charge with time, $\Delta Q_{E1}/\Delta t$. Allowance must therefore be made for any oxidation that occurred during the adsorption step itself, *e.g.*, immediate oxidation of dissociated hydrogen. This may be done by multiplying $\Delta Q_{E1}/\Delta t$ by the ratio of the charge associated with oxidation of the hydrocarbon fuel molecule to that required for oxidation of the adsorbed species.

While the precise composition of the ad-layer has not been established for either methane or ethane, especially after short equilibrations, it is possible to calculate a range of limiting currents from the initial adsorption data at 0.3 and 0.4v. In the case of methane, depending on whether the ad-layer is assumed to have an average composition approaching that of methyl radicals or that of a highly oxygenated species, such as CO, the observed rate of adsorption would be equivalent to a steady state current density of from 0.30 to 1.2 μa/cm² of real area. The observed value of 0.3 μa/cm² is in good agreement in view of the evidence for a mixture of C_1 radicals and partially oxygenated species.

A similar calculation has been made for ethane (3). In this case the calculated maximum current density fell in a range from 14 to 35 μa/cm² and the observed value was 2.5 $\mu a/cm^2$ of real area. For comparison, Rhodes (16) obtained adsorption rates equivalent to 22 $\mu a/cm^2$ (10^{13} molecules/cm²/sec) for ethane on a rotated platinum electrode (600 rpm) at 80°C with a $1N$ H_2SO_4 electrolyte. While this value is in excellent agreement with the results with the Teflon bonded electrode, no data were obtained for the steady-state maximum current obtainable with the rotating electrode.

The discrepancy between the calculated and observed maximum current densities for ethane on the Teflon-bonded electrode undoubtedly reflects the fact that at the potential of the maximum steady-state current some of the more refractory species are present on the surface and lower the adsorption rate relative to that on the "clean" surface at 0.3v. The decline in the current density that occurs at higher potentials appears to reflect further reductions in adsorption rate as a result of such processes as surface oxidation, anion adsorption, and stronger bonding of water to the surface. These processes would also contribute to the similar decline in methane performance at potentials above 0.5v.

At low potentials, the effect of the adsorption rate on the polarization curve is minimal. Here it is clear that the overvoltage required for the further oxidation of surface intermediates to CO_2 is limiting. This is true, of course, under potentiostatic conditions as well as with the resistive loads of practical fuel cells.

The pronounced temperature coefficients for both the methane and ethane adsorptions (activation energy of about 14 kcal/mole) are reflected in the observed improvement in the performance of hydrocarbon fuel cells with increasing temperature. In particular, they relate to the regions of "unstable" performance observed with saturated hydrocarbon fuel cells operating on resistive load (17-19). Under these conditions, it will be recalled that at low current densities steady performance is obtained while at higher current densities the performance decays with time or, under certain conditions, oscillations set in (19, 20). As a result of the increasing adsorption rates with increasing temperature, the region of instability occurs at continuously higher current densities as the operating temperature is increased. When polarization curves are obtained potentiostatically, as in the present work, maximum currents are observed in place of the instability associated with resistive loads.

While it would be premature to discuss the mechanisms of the electrode reactions in any detail at this time, it is appropriate to consider briefly some of the possible paths suggested by the available information. In particular it is pertinent to speculate about the meaning of the two separate l.a.s. waves seen with ethane and propane, the single wave seen with methane, and the evidence for the partially oxidized surface species. In the discussion that follows, ethane will be used as the model with the expectation that higher molecular weight hydrocarbons will behave similarly. The behavior of methane, in turn, will be somewhat simpler.

The initial step must certainly involve adsorption of the fuel on the electrode surface. On the basis of careful kinetic studies with ethane on wire microelectrodes, Gilman has concluded (1, 2) that this primary adsorption step corresponds to the formation of an ethyl radical on the surface. This may be represented by

$$C_2H_6\,(\text{gas})^2 + S \rightarrow S - C_2H_5 + H^+ + e \qquad [2]$$

at potentials at which appreciable currents are drawn from the electrode. He points out that an equivalent route is given by

$$C_2H_6\ (\text{gas}) + 2S \rightarrow S - C_2H_5 + S - H \qquad [2a]$$

[2] More precisely, the gas will first dissolve in the electrolyte and be transported by diffusional processes to the electrode where it will adsorb from solution. While mass transport processes are not limiting in the work under discussion, it is obvious that they can become important under some conditions of operation. For practical fuel cell electrodes it is important that mass transport limitations be minimized.

in which case the adsorbed hydrogen is rapidly consumed by the Volmer reaction:

$$S - H \rightarrow S + H^+ + e \qquad [2b]$$

At low potentials, of course, some of the hydrogen will remain adsorbed on the surface.

Gilman then reasons that the ethyl radical follows two paths. The first results in the formation of four surface bonds to the surface without rupture of the C-C linkage

$$S - C_2H_5 + 3S \rightarrow S_4 - C_2H_2 + 3H^+ + 3e \qquad [3]$$

This species is associated with wave 2 obtained with a l.a.s. and is identical with the single adsorbed species obtained when ethylene and acetylene are adsorbed (2). The present work is in accord with this interpretation, and cathodic hydrogenations of adsorbed ethane at 25°C have shown that the major material on the surface at that temperature corresponds to C_2 species while that for propane corresponds to C_3 species (12).

The second reaction path of the ethyl radical results in the formation of the material associated with wave 1, which Gilman also obtained for ethane on the platinum wire microelectrode. In the absence of detailed kinetic data for the species associated with wave 1 Gilman did not speculate in detail on its identity.

The new data obtained with the Teflon-bonded electrodes are helpful in this area. The similarities between the single wave for methane and wave 1 for ethane, as well as other evidence noted above, strongly suggest that the second reaction path of the ethyl radical involves C-C bond fission as indicated in the following general equation

$$S - C_2H_5 + S \rightarrow 2S - CH_a + (5 - 2a)\ H^+ + (5 - 2a)\ e \qquad [4]$$

(The methylene radical with two carbon bonds to the surface may represent the principal species in parallel with the C_2H_2 of wave 2 which also has two surface bonds per carbon atom.)

The C_1 species in turn appear to react readily with water to form a partially oxygenated material which corresponds to the previously proposed "CO-like" species of Niedrach (12) and the "reduced CO_2" of Giner (21), and which Giner has also more recently found to be formed during the oxidation of hydrocarbons in the presence of a sulfuric acid electrolyte (22). Brummer and Turner (8) have also obtained evidence for the presence of partially oxygenated surface species in their studies of propane at higher temperatures with a phosphoric acid electrolyte, as have Niedrach and Tochner (7).

The specific identity of the oxygenated species is as yet unknown and the reaction can therefore best be represented by

$$S - CH_a + b\,H_2O + cS \rightarrow S_{(c+1)} - CH_dO_b + (a + 2b - d)\ H^+ + (a + 2b - d)\ e \qquad [5]$$

That both the C_1 species and the partially oxygenated species are present on the surface and oxidize over the same potential range is indicated by the new hydrogenation experiments with methane and ethane. Since Eq. [4] represents a "cracking" reaction and Eq. [5] a "reforming" reaction, these observations suggest that it would be profitable to direct attention toward the study of the behavior of alternative catalysts in promoting such reactions.

With regard to the more refractory species of wave 2, which oxidize only at higher potentials, it is likely that an entirely different mechanism of oxidation prevails. This conclusion is based on Gilman's observation that conversion to the species of wave 1 is slow (2). It is therefore likely that oxidative attack occurs before the C-C bonds are ruptured. This could result in the formation of alcohol-like species as intermediates. It should be emphasized, however, that such intermediates will undoubtedly be quite distinct from those involved in the direct oxidation of alcohol-type fuels at moderate temperatures. The alcohol-like species derived from hydrocarbons would be strongly bound to the surface by multiple carbon-metal linkages, and hence complete oxidation to CO_2 would be assured. With alcohol fuels it is more likely that weaker bonds between the oxygen and the metal are involved. This is suggested by the incomplete oxidation to organic acids that is often observed with alcohols (23) at moderate temperatures. It is further supported by the behavior of alcohols towards deuterium exchange, where it is found that the hydroxylic hydrogen undergoes exchange most readily (24).

Relating to the oxidation of these multiple-carbon species is the work of Bockris and co-workers (25-27) dealing with the oxidation of ethylene and acetylene. They interpret Tafel plots and other evidence in terms of a slow step involving the production of hydroxyl radicals from water. Such a route would not be in conflict with the present results.

Summary and Conclusions

The behavior of methane on Teflon-bonded fuel cell electrodes parallels that of ethane in that adsorption at intermediate potentials varies linearly with time at low coverages, and a semilogarithmic relationship applies at higher coverages. Rates of adsorption of methane are, however, over an order of magnitude lower than those previously observed with ethane. At 65°C the measured rate of adsorption of methane on a "clean" surface correlates well with the maximum anodic current that can be drawn from the electrode. This is in marked contrast to the behavior of ethane where the observed maximum current is almost an order of magnitude lower than that calculated from the adsorption rate. The difference in behavior of the two fuels is related to the ad-layers formed during adsorption. In the case of methane only readily oxidized C_1 species, some of which are partially oxygenated, form. The ad-layer from ethane also contains relatively refractory C_2 species which block the surface and limit the adsorption rate at the potential of the maximum current.

On the basis of the behavior of methane and ethane it is possible to construct a tentative picture of the steps involved in the anodic oxidation of hydrocarbons on platinum catalyzed fuel cell electrodes. After a primary adsorption step, at least two distinct reaction paths are followed by ethane and higher hydrocarbons. One path results in the formation of the relatively refractory species. The most desirable path results in "cracking" of the carbon chain to form the more reactive C_1 radicals and the partially oxygenated species. At low current densities the overvoltage associated with oxidation of the ad-species to CO_2 limits performance. As the current density is increased the adsorption rate eventually becomes the limiting factor.

In view of the many species present on the electrode surface and the changes in coverage and composition with temperature, potential, and time, much attention to analytic detail will be required before a definitive mechanism can be derived. It seems unlikely that electrochemical measurements alone will be sufficient to unravel all of the steps. Instead, much supplementary information must be sought, particularly with regard to the identification of surface species and their roles as active intermediates or passive byproducts. Radiotracer, infrared, chromatographic, and other related techniques should prove invaluable in identifying such species, in measuring "turnover" rates on the electrode surface, and in providing additional supporting information.

Acknowledgments

The author is indebted to S. Gilman for many helpful discussions.

This work is a part of the program under contracts DA-44-009-AMC-479(T) and DA-44-009-ENG-4909, ARPA Order No. 247 with the U. S. Army Engineer Research and Development Laboratories, Ft. Belvoir, Virginia, to develop a technology which will facilitate the design and fabrication of practical military fuel cell power plants for operation on ambient air and hydrocarbon fuels.

Manuscript received Nov. 18, 1965; revised manuscript received April 6, 1966.

Any discussion of this paper will appear in a Discussion Section to be published in the June 1967 JOURNAL.

REFERENCES

1. S. Gilman, *Trans. Faraday Soc.*, **61**, 2546, 2561 (1965); **62**, 466, 481 (1966).
2. S. Gilman, in "Hydrocarbon Fuel Cell Technology," p. 349, B. S. Baker, Editor Academic Press, New York (1965).
3. L. W. Niedrach, S. Gilman, and I. Weinstock, *This Journal*, **112**, 1161 (1965).
4. L. W. Niedrach and H. R. Alford, *ibid.*, **112**, 117 (1965).
5. S. Gilman, *J. Phys. Chem.*, **67**, 78 (1963).
6. F. G. Will and C. A. Knorr, *Z. Elektrochem.*, **64**, 258 (1960).
7. L. W. Niedrach and M. Tochner, To be published.
8. S. B. Brummer and M. J. Turner, in "Hydrocarbon Fuel Cell Technology," p. 409, B. S. Baker, Editor, Academic Press, New York (1965).
9. H. Dahms, M. Green, and J. Weber, *Nature*, **195**, 1310 (1962).
10. E. Gileadi, B. T. Rubin, and J. O'M. Bockris, *J. Phys. Chem.*, **69**, 3335 (1965).
11. R. J. Flannery and D. C. Walker, in "Hydrocarbon Fuel Cell Technology," p. 335, B. S. Baker, Editor, Academic Press, New York (1965).
12. L. W. Niedrach, *This Journal*, **111**, 1309 (1964).
13. W. T. Grubb, *ibid.*, **111**, 1086 (1964).
14. D. W. McKee, *J. Phys. Chem.*, **67**, 841 (1963).
15. B. E. Knox and H. B. Palmer, *Chem. Rev.*, **61**, 247 (1961).
16. D. R. Rhodes, Paper presented at the Washington Meeting of the Society, October 1964, Extended Abstracts of the Battery Division, p. 36.
17. W. T. Grubb, Proc. 16th Annual Power Sources Conference, Atlantic City, N. J., p. 31 (1962).
18. L. W. Niedrach, *This Journal*, **109**, 1092 (1962).
19. M. J. Schlatter, *Advan. Chem. Ser.*, **47**, 292 (1965).
20. H. Binder, A. Köhling, H. Krupp, K. Richter, and G. Sandstede, *This Journal*, **112**, 355 (1965).
21. J. Giner, *Electrochim. Acta*, **8**, 857 (1963).
22. J. Giner, 15th Meeting CITCE, London and Cambridge, September 21-26, 1964, summaries of papers, p. xxix.
23. H. Binder, A. Köhling, and G. Sandstede, *Advan. Chem. Ser.*, **47**, 283 (1965).
24. G. C. Bond, "Catalysis by Metals," p. 220, Academic Press, New York (1963).
25. M. Green, J. Weber, and V. Drazic, *This Journal*, **111**, 721 (1964).
26. J. W. Johnson, H. Wroblowa, and J. O'M. Bockris, *ibid.*, **111**, 863 (1964).
27. H. Wroblowa, B. J. Piersma, and J. O'M. Bockris, *J. Electroanal. Chem.*, **6**, 401 (1963).